Chapter 14
Electrospun Carbon-Based Nanocomposites as Anodes for Lithium Ion Batteries

Apurva Patrike, M. Thripuranthaka, Golu Parte, Indrapal Karbhal, and Manjusha Shelke

14.1 Introduction

With increasing population, demand for energy sources is increasing globally because of insufficient fossil fuel. In the context of increasing energy demand, clean and efficient energy conversion and high capacity energy storage are becoming an urgent task. Rechargeable lithium ion batteries (LIB) are one of the promising electrochemical storage devices due to its high energy density and long working life. Hence, LIB has gained intense attention from academic community as well as industry in commercialization point of view. LIB technology has dominated in portable electronic market in past two decades. Nowadays, these are intensively used in transportation application like hybrid electric vehicles (HEV), electric vehicles (EV) and in stationary energy storage application like grid storage technology. Considering huge demand for energy and power density, tremendous research has been devoted on LIB to improve its electrochemical performance. The electrochemical performance of LIB including high capacity, high energy density, operation potential and current densities with longer working life is mainly depending on electrode materials [1, 2]. State-of-the-art LIB utilizes Li containing metal oxides/phosphates as cathode and graphite as anode material. Electronic and ionic conductivity are the two crucial factors for any material which is considered to be electrode material for LIB. These two parameters can be improved through doping, nanostructure engineering and carbonaceous material addition [3].

A. Patrike · M. Thripuranthaka · G. Parte · I. Karbhal · M. Shelke (✉)
B101, Polymer and Advanced Materials Laboratory Physical & Material's Chemistry Division, CSIR-National Chemical Laboratory, Pune, India
e-mail: mv.shelke@ncl.res.in

Academy of Scientific and Innovative Research (AcSIR), Ghaziabad 201002, UP, India

At present, graphite is used as anode in commercial LIB with limited capacity ($372 \, \text{mAh g}^{-1}$) and long Li^+-ion diffusion path. Tremendous efforts have been taken to explore new materials as an anode for LIB. Out of which the number for carbon-based materials is more as carbon has promising properties like low cost, safety, easy availability and also it has been conventionally utilized in commercial LIBs. However, the development of new carbon materials is at most important in order to meet requirement of ever increasing energy demand, growing number of electronic devices and large-scale applications for stable electrochemical performance in LIB.

Recently, the number of carbon materials with different nanostructures has been explored as an anode for LIB like graphene [4], carbon nanotubes [5], carbon nanofibers [6], etc. Out of which carbon nanofibers attracted more attention due to its one-dimensional (1D) nature which provides favorable properties for electrochemical storage of Li^+-ions in LIB. CNF provides good access for electrolyte due to enhanced surface-volume ratio and conductivity along the length. In high surface area, CNF provides shorter path for Li insertion, efficient 1D electron transport along length compared to powder materials which ultimately gives lower resistance and high capacity [7, 8].

Several methods have been employed for CNF synthesis like catalytic synthesis [9], electrospinning technique [10], chemical vapor deposition growth [11] and template-based methods [12]. Out of which the electrospinning technique is simple, versatile and cost effective. It can be used from laboratory level synthesis to industry level large-scale synthesis to prepare various CNFs and its composites. Electrospinning provides an advantage of synthesis of continuous CNFs with controllable morphology, porous CNFs, core-shell CNFs and metal loading into CNFs [13]. Diameter of CNFs produced from electrospinning technique varies from few nanometers to few hundred nanometers.

14.1.1 Working Principle of Electrospinning

This technique uses precursors dissolved in suitable solvent as starting material to draw nanofibers through application of high electric potential (several kV range). The high voltage is applied between the needle of syringe comprised of precursor solvent and metallic plate which is used to collect nanofibers (collector) and is grounded. With instrumental parameters like voltage, distance between syringe and metal collector, flow rate of precursor solvent and viscosity of solvent, one can adjust diameter and length of nanofibers. The shape of collector also plays an important role and there are two types of collectors, viz., plate collector and drum collector. Nanofibers collected on plate collector are not orientated in a particular direction, whereas drum collector provides orientated nanofibers aligned in a particular direction. Hence, the synthesis of nanofibers with desired physical properties is achieved in electrospinning technique [10]. Schematic of electrospinning technique with different collector is shown in Fig. 14.1.
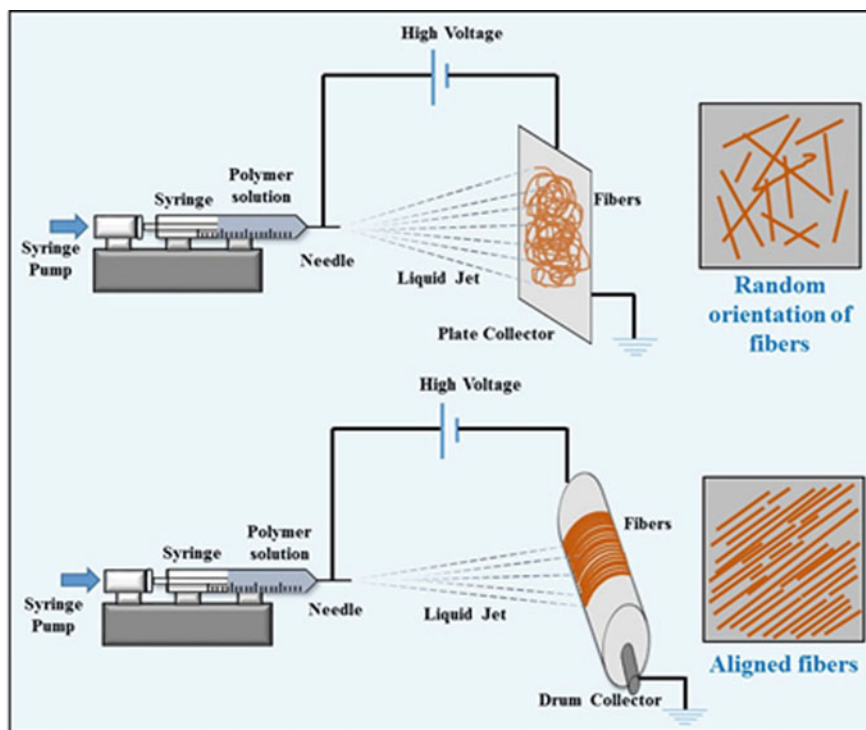
Fig. 14.1 Schematic of electrospinning technique with plate and drum collector

The current chapter emphasizes on electrospun carbon nanofibers as anode materials for LIB including recent trends, scientific developments and strategies to improve electrochemical performance of CNF and detailed synthesis protocols. Moreover, it covers the importance of composites of CNF for better performance.
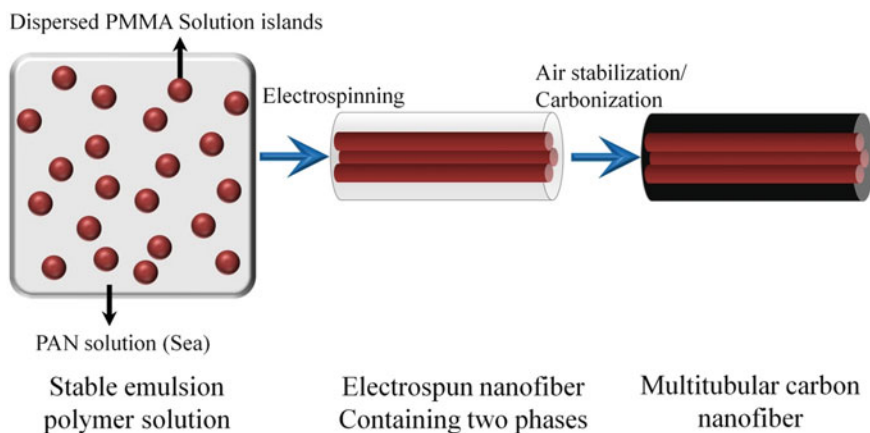
14.2 Electrospun Fibers

14.2.1 Solid Fibers

Various synthetic and natural polymers have been utilized for synthesis of CNFs via electrospinning technique. The commonly used polymers are polyvinyl alcohol (PVA) [14], polyvinyl pyrrolidone (PVP) [15], polyacrylonitrile (PAN) [16] and cellulose [17]. The physical and chemical properties of CNF are determined by the precursor. Out of these PAN has been extensively used as carbon precursor as it has good spinnability property and can yield good amount of carbon after stabilization and carbonization process. Synthesis of PAN-based CNFs is performed in three stages

which are electrospinning, stabilization of polymer and carbonization. CNFs derived from PAN possess robust structure and good electrical conductivity. Hence, the direct use of CNF web can be employed as an anode for LIB which avoids the use of polymer binder and conducting additives which ultimately reduces weight of LIB cell [18]. Yang et al. [18] has synthesized N, P and Si tridoped nonporous carbon nanofibers with increased N content in carbon matrix to use it as electrode for supercapacitor. This nonporous structure has demonstrated to find out heteroatom doping amount in carbon matrix with enhanced rate capability and specific capacitance.

14.2.2 Porous Fibers

Incorporation of porous structure in CNFs increases specific capacitance and rate performance for LIB. This is attributed to interconnected particles which enhances surface for charge transfer and better electrode–electrolyte interaction. Various strategies have been utilized to make porous CNFs. Chan Kim et al. [19] have synthesized porous carbon fibers via electrospinning technique with two stable and immiscible polymer solutions and thermal treated at 1000 °C. Use of two immiscible polymer solutions utilized to control the pore size and surface area of nanofibers by changing the blend proportions in different ratios. The schematic diagram and electron microscopy images are shown in Figs. 14.2 and 14.3, respectively.

Fig. 14.2 Schematic diagram of procedural steps involved in synthesis of porous nanofibers. Adapted and reproduced from Ref. [19], Copyright 2007 John Wiley and Sons
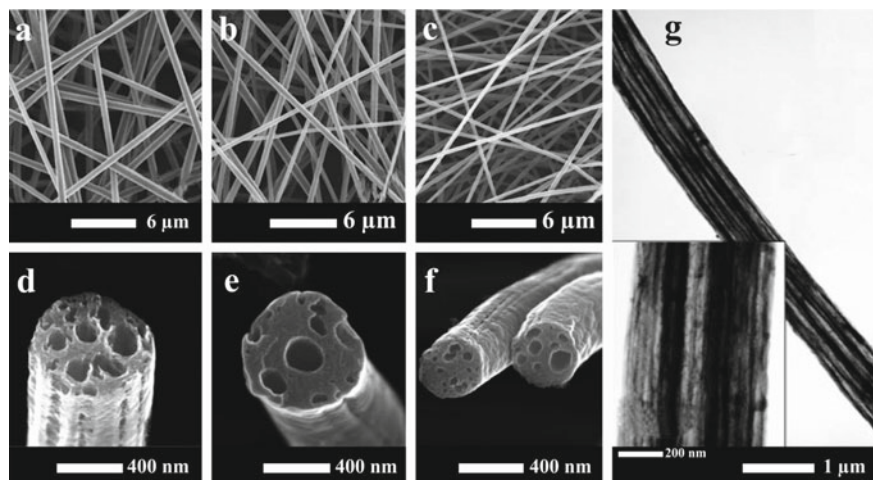
Fig. 14.3 a, **b**, **c** Morphology of electrospun nanofibers comprising of two polymer phases. PAN:PMMA **a** 5:5, **b** 7:3 and **c** 9:1. **d**, **e**, **f** Cross-sectional FESEM images of thermally treated nanofibers at 1000 °C with similar PAA:PMMA ratios 5:5, 7:3 and 9:1, respectively, **g** TEM images of 5:5 PAN:PMMA sample. The inset is a magnified TEM image. Adapted and reproduced from Ref. [19], Copyright 2007 John Wiley and Sons

14.2.3 Core-Shell/Co-axial Fibers

In certain cases, the functionalization of nanofibers over surface through functional coatings or particles is required to fulfill the requirements. Electrospinning technique is a versatile technique for fabrication of such fibers. This involves spinning of two different polymers precursor solutions via concentrically aligned nozzles. Same potential is applied to spin the fibers and the thickness of shell can be maintained by flow rate of precursor solution. Depending on requirements, materials for shell and core are decided [20]. Yang et al. [21] fabricated hollow CNF from PAN with styrene-co-acrylonitrile (SAN) polymer as sacrificial core materials and later it is filled with Si nanoparticles. These Si nanoparticles stuffed CNFs help to control volume expansion of Si during lithiation/de-lithiation process, and CNFs matrix over the surface of Si provides mechanical support path lengths for charge transfer. TEM images of hollow CNF and Si encapsulated hollow CNFs are shown in Fig. 14.4.

14.3 Synthesis of CNF from Different Precursors

Carbon nanofibers can be synthesized by different methods such as vapor growth, chemical vapor deposition, laser ablation, arc discharge and electrospinning. Among these, electrospinning provides a simple and scalable process for the production
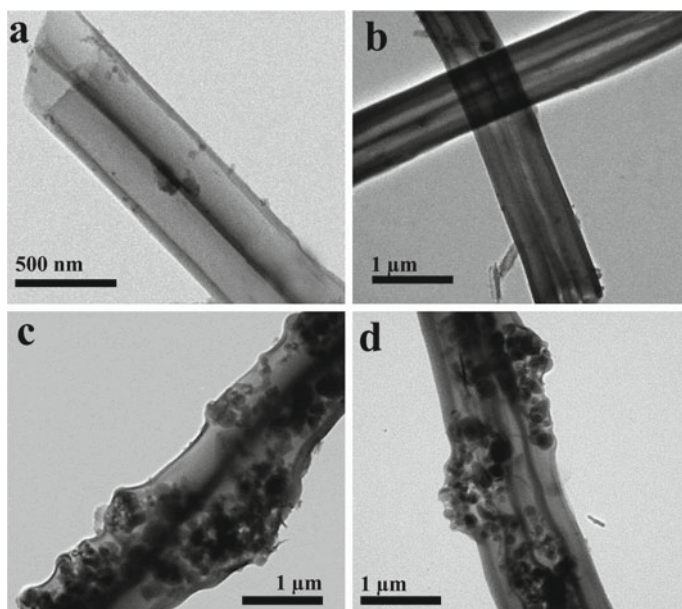
Fig. 14.4 Transmission electron microscopy (TEM) images of **a** two-channeled hollow CNF, **b** four-channeled hollow CNF, **c** Si encapsulated two-channeled hollow CNF and **d** Si encapsulated four-channeled hollow CNF. Adapted and reproduced from Ref. [21], Copyright 2014 Royal Society of Chemistry

of carbon nanofibers. In typical CNF synthesis, electrospinning of polymer solution followed by stabilization and carbonization of electrospun polymer fibers into CNFs. Various factors determine the structure and properties of the electrospun CNFs which includes (1) solution properties like polymer, concentration, electrical conductivity and surface tension; (2) processing conditions such as strength of applied electric field, flow rate of polymer solution and distance between the spinneret and the collector. Along with these, surrounding temperature and humidity also affect the morphology and properties of CNFs. CNFs can be prepared by any material having carbon chain. Although the variety of polymer precursors have been electrospun for the CNF synthesis, commonly used polymers are PAN, PVA, polyimide, PVdF, PVP and phenolic resins have been used for the synthesis of electrospun CNF. The electrospinning parameter and polymers employed for the synthesis of carbon nanofibers by various research groups have been described here.

PAN has been extensively used to get the electrospun CNFs due to its high carbon yield, easy processing and mechanical stability of synthesized carbon nanofibers. Kim et al. developed carbon nanofibers web (CNFW) from PAN as a carbon precursor. Electrospinning solution was prepared by dissolving PAN in DMF. Electrospun carbon fibers were stabilized at 280 °C in air for 1 h and further carbonized

at 1000 °C in inert atmosphere to obtain carbon nanofibers web. The structural variations of CNFW with different heat treatment temperatures (700–2800 °C) were studied [22–24].

Despite the enormous success of PAN as carbon precursor for the CNF synthesis, its solubility in many solvent is relatively low. DMF is most used as solvent to make electrospinning solution of PAN. To counter this problem, P. Wang and coworker used PVP as carbon precursor for the CNF synthesis as its solubility is better in solvent, including water and ethanol, cheaper than PAN and environmentally benign. PVP was dissolved in ethanol to prepare precursor solution for electrospinning. The electrospun nanofibers were stabilized at 150 °C for 24 h in air and pre-oxidized for 4 h at 360 °C and annealed in N_2 atmosphere at 800 °C for 4 h to produce CNFs and investigated as an electrode material for Li-ion battery [15]. Figure 14.5 shows the SEM images of PVP synthesized CNFs. Dong et al. [25] used PVP as a carbon precursor in DMF to synthesize carbon nanofibers via electrospinning. The electrospun PVP nanofibers were stabilized at 300 °C for 3 h and then annealed at 500 °C in argon atmosphere for 3 h to obtain CNF. The PVP synthesized CNFs was doped with cobalt and used as an electrode material for Li-ion battery.

PVA, another water soluble polymer also studied as a carbon precursor for the synthesis of CNFs. Although PVA does not withstand high temperature and gives low carbon yield, Ding et al. [26] synthesized PVA cross-linked carbon nanofibers to study the factors that affect the morphology and porosity of PVA CNFs. The morphology mostly influenced by solution concentration and applied voltage. Some
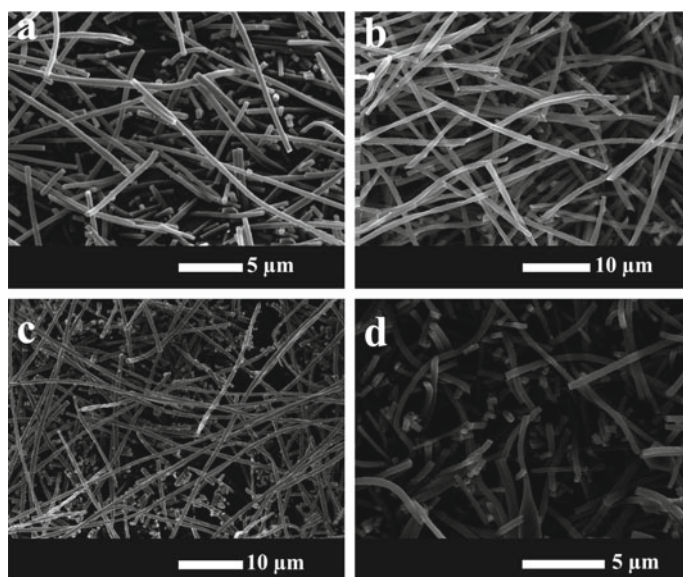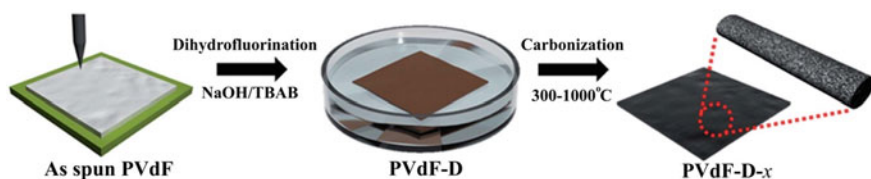

Fig. 14.5 SEM images of PVP synthesized CNFs. Adapted and reproduced from Ref. [15], Copyright 2012 Royal Society of Chemistry

other reports are on PVA as carbon precursor for the CNFs synthesis. W. K. Sun studied the effect of pH on electrospinning of poly(vinyl alcohol). They found that in acidic condition CNFs are not continuous [14, 27].

Hong et al. produced porous CNFs prepared from PVdF for CO_2 capture. They dissolved PVdF in mixture of acetone and N, N-dimethylacetamide to form 11% PVdF solution. This solution was electrospun to get nanofibrous mat, which dehydrofluorinated to stabilize the CNFs and then carbonized for 1 h in the temperature range of 300–1000 °C to obtain porous carbon nanofibers. Various other papers are also available for the synthesis of PVdF-based CNFs for Li-ion batteries. Figures 14.6 and 14.7 show the schematic and representative SEM images of PVdF synthesized CNFs, respectively [28–31].

For the manipulation of morphology and porosity in CNFs, mainly two strategies have been employed sacrificial and activation methods. Different nanostructures such as SiO_2, nano-$CaCO_3$ or polymers such as PVA, polymethyl methacrylate (PMMA), PVP, poly (ethylene oxide), Nafion, polysulfone, polystyrene, poly-L-lactic acid have been introduced during polymer precursor solution preparation as a sacrificial component. By thermal or chemical treatments, these sacrificial components (i.e., nanostructures or polymer) extracted from the electrospun fiber that helps in creating porosity.

Fig. 14.6 Schematic for synthesis of PVdF-based CNFs. Adapted and reproduced from Ref. [28], Copyright 2014 Royal Society of Chemistry
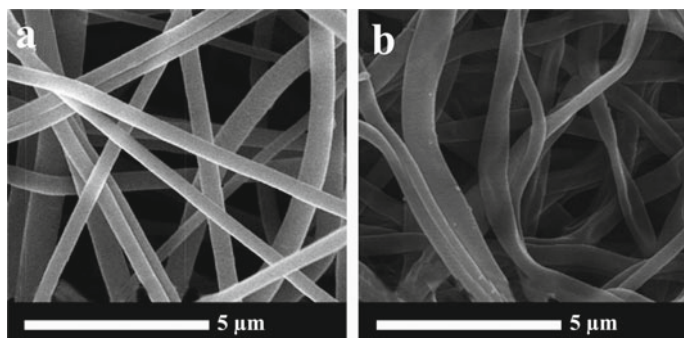

Fig. 14.7 SEM images of synthesized PVdF-based CNFs. Adapted and reproduced from Ref. [28], Copyright 2014 Royal Society of Chemistry

L. Ji and coworker prepared porous carbon nanofibers by adding SiO_2 as porogen in PAN/DMF precursor solution. The electrospun PAN/SiO_2 composite nanofibers were then stabilized at 280 °C and then carbonized at 700–1000 °C in N_2 atmosphere for an hour to get carbon/SiO_2 composite nanofibers. By HF treatment, SiO_2 nanoparticles were removed to create porous carbon nanofibers [32, 33]. Zhang et al. prepared hierarchical porous carbon nanofibers by electrospining a polymer solution composed of polyacrylonitrile (PAN) and nano-$CaCO_3$ in DMF. They first dispersed nano-$CaCO_3$ in DMF/THF and then added PAN to make polymer precursor solution [34].

Numerous papers have been reported on the preparation of bicomponent polymer fibers comprising PAN as primary carbon precursor and integration of sacrificial polymers in PAN/DMF solution. These composite nanofibers get stabilized during carbonization by molecular interaction between the both the polymers.

Peng et al. reported electrospinning of 12 wt% PAN/PMMA bicomponent polymer precursor in DMF. The stabilization was carried out at 250 °C in air for 6 h followed by carbonization at 800 °C for 1 h in N_2 atmosphere to obtain porous CNF. The PAN without PMMA showed long and bread-free morphology while with PMMA it forms interconnected network. This is due to melting of PMMA during carbonization which leads to fibers-fiber connection. Figure 14.8 shows the representative SEM images of PAN and morphology development with addition of PMMA in PAN synthesized CNFs. Several other papers have been reported to improve the fiber structure and morphology by adding thermally liable polymer [35–39].
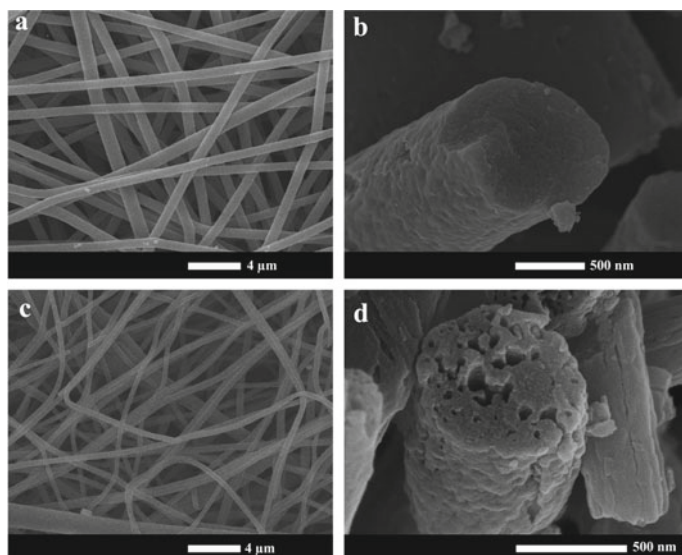
Fig. 14.8 SEM images of PAN/PMMA-based CNFs. Adapted and reproduced from Ref. [35]. Copyright 2015 Springer Nature
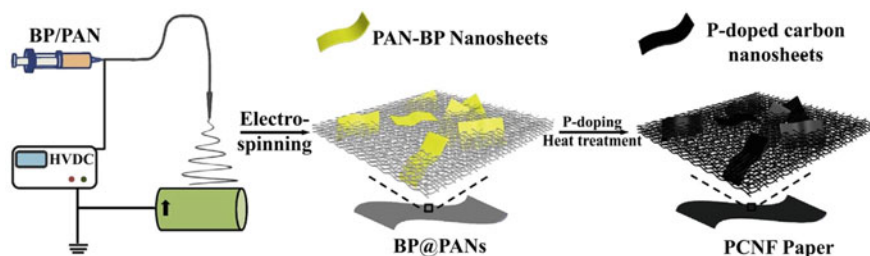
Fig. 14.9 Schematic illustration of preparation of PCNF paper. Adapted and reproduced from Ref. [43], Copyright 2018 Elsevier

Heteroatom (e.g., boron, nitrogen, sulfur and phosphorus) doping in carbon material is an effective way to tailor their electronic and chemical properties. These doping enhances the electrochemical performance of the materials. Nan et al. synthesized N-doped carbon nanofibers using PAN and melamine. In this, the solution concentration of 10 wt% PAN in DMF was prepared and melamine was added in the 2:1 ratio of PAN/DMF: melamine. This solution was electrospun and stabilized at 250 °C for an hour and carbonized at 850 °C for 1 h to obtain nitrogen-doped carbon nanofibers networks. These fibers further activated by 20% ammonia in N_2 atmosphere to get N_2-rich carbon nanofibers [40–42].

Li et al. reported the phosphorus-doped carbon nanosheets/nanofibers freestanding paper from PAN as carbon precursor in DMF, and subsequently black phosphorus/red phosphorus was added to form electrospun solution. The obtained electrospun fibers annealed at 800 and 900 °C in N_2 atmosphere for 1 h to form carbon nanosheets/nanofibers. Phosphorus enhances the electrocatalytic activity of carbon fibers. Figure 14.9 shows the schematic of synthesis of P-doped carbon nanosheets/nanofibers [43].

From the given synthesis protocols, it is evident that the electrospinning has emerged as a promising technique for the synthesis of carbon nanofibers from variety of polymers. The morphology and structure properties of electrospun nanofibers can be modified and controlled in number of different chemical or physical methods. These nanofibers material have been utilized in large number of applications such as catalysis, sensors, biomedical, adsorption, energy conversion and storage applications.

14.4 CNF-Based Nanomaterials as Anode for LIB

Electrospun carbon nanofibers are attracted toward energy storage application due to unique 1D physical and chemical property. Long fiber length of CNF provides easy

access for Li$^+$-ions to the innermost area of anode. CNFs are extensively researched as an anode for lithium ion batteries. Some of the selected research works are discussed in this section of chapter.

14.4.1 CNF-Based Anode

C. Kim et al. have synthesized CNF from PAN polymer from electrospinning followed by stabilization at 260 °C in air and thermally treated at 1000 °C in inert atmosphere. Further, this CNF has shown high capacity of 435 mAh g^{-1} at 30 mA g^{-1} after two cycles. The authors elaborated the detail study of temperature (700, 1000 and 2800 °C). The study shows that CNF prepared at 1000 °C exhibited highest electrochemical performance as interlinked CNF provides high electrical conductivity [44]. Utilization of electrospinning parameters comes with improved capacity by tuning CNF in different morphology and incorporation of other active materials. One of such strategy was incorporated to make porous hollow CNFs (pHCNFs) via co-axial electrospinning by Lee et al. Improved electrochemical performance for pHCNFs is elaborated by authors where styrene-co-acrylonitrile (SAN) was used as sacrificial material for core and for porosity generation on shell of PAN-based HCNF. pHCNFs were obtained after subsequent heat treatments where SAN get decomposed and burnt. Improved LIB performance was obtained for porous pHCNFs as porous nature of CNFs improves intecalation/de-intercalation mechanism. Initial discharge capacity for pHCNFs and HCNFs was 1003 mAh g^{-1} and 653 mAh g^{-1}, respectively, at 50 mA g^{-1}. The initial capacity at 200 mA g^{-1} was reduced to 827 mAh g^{-1} for pHCNFs. This is because at high current rates, intercalation gets disturbed. The schematic and battery performance for the same is shown in Fig. 14.10(a) and Fig. 14.10(b) respectively [45].
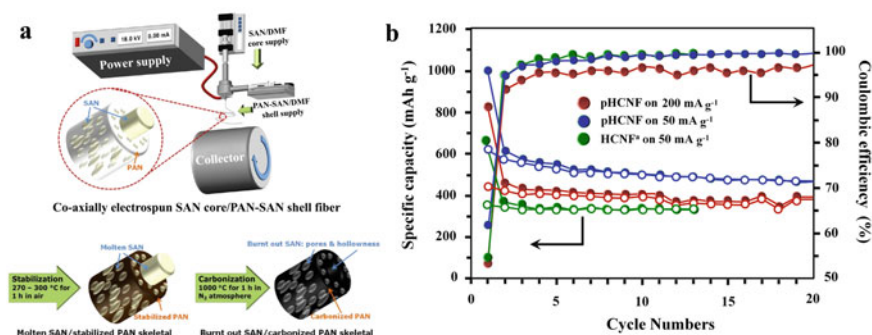

Fig. 14.10 (**a**) Schematic for synthesis of pHCNFs. (**b**) Battery performance. Adapted and reproduced from Ref. [45], Copyright 2012 American Chemical Society

To tailor electronic and chemical properties of CNFs, chemical doping into carbon with heteroatom is an effective and beneficial strategy. Many dopants have been used for improvement in conductivities like nitrogen [46], phosphorous [47], boron [48] and sulfur [49]. Among these, the nitrogen is an effective dopant as it has atomic radius (56 pm) similar to carbon (67 pm) and has more electronegativity (3.04) as compared to that of carbon (2.55). N doping gives following benefits to carbon: (1) As N has lone pair of electrons, it can introduces donor states which gives n-type conducting nature, (2) N can easily bond with carbon and this helps for easy Li^+-ion insertion [50], (3) N introduces defect sites in carbon which improves Li^+-ion storage reservoir sites [40]. Based on these, in order to achieve high performance for LIB with good rate capability, high capacity and long cycling stability, N doping to porous carbonaceous material is highly desirable. D. Nan et al. developed N enriched porous CNF through electrospinning method as free-standing anode for LIB application as shown in Fig. 14.11a. Typical synthesis procedure involves PAN and melamine as precursors for carbon and nitrogen. Porous N enriched CNFs (NPCNFs) were achieved after stabilization and NH_3 treatments of electrospun fibers. TEM image of NPCNFs is shown in Fig. 14.11b. NPCNFs showed high initial capacity of 1323 and 1150 mAh g^{-1} after 50 cycles at 50 mA g^{-1} current density value as shown in Fig. 14.12a. It indicates that N doping in porous CNFs provided much improved Li^+-ion storage performance with good rate capability (Fig. 14.12b) as compared to nonporous and without doped CNFs [39].

Moreover, the phosphorous doping also contributes to improve electronic and chemical properties of carbon. Li et al. developed phosphorus-doped carbon nanosheets/nanofibers via electrospinning and subsequent heat treatments to use it as anode for LIB. The electrode was fabricated in flexible and free-standing form which allows complete utilization of active material in electrochemical tastings. These types of free-standing flexible electrodes are need for the next generation flexible batteries. Black phosphorus (BPCNF) and red phosphorus (RPCNF) doping in carbon nanosheets/nanofibers are demonstrated in this work. With BP doping electrochemical performance got improved as compared to RPCNF and CNF, this could be due to enhancement in electrical conductivity and electrochemical reactivity of
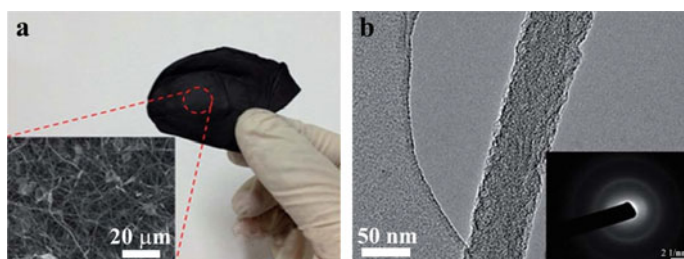

Fig. 14.11 a Free-standing electrode images with microscope image in inset, **b** TEM of NPCNF with SAED pattern in inset. Adapted and reproduced from Ref. [40], Copyright 2014 Royal Society of Chemistry
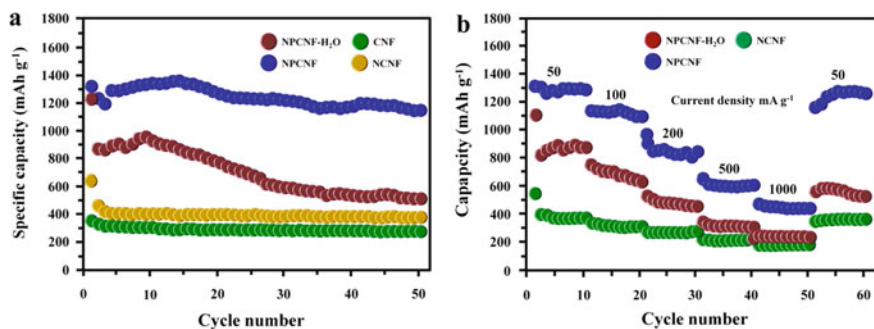
Fig. 14.12 **a** Cycling stability at 50 mA g^{-1} current density and **b** rate performance of different samples. Adapted and reproduced from Ref. [40], Copyright 2014 Royal Society of Chemistry

carbon upon doping with BP. Among all allotropes of phosphorus, BP is thermodynamically stable one which provides high P doping during thermal treatment. This is attributed to improved capacity value for BPCNF as compared to RPCNF and CNF as shown in Fig. 14.13. At 1 A g^{-1} current density, after 700 cycles capacity values for BPCNF-800, RPCNF-800 and CNFs are 607 mAh g^{-1}, 356 mAh g^{-1} and 192 mAh g^{-1}, respectively, where 800 indicates annealing temperature of electrospun nanofibers. The self-supporting flexible CNF electrode accommodated volume changes during lithiation/de-lithiation as well as provided conductivity to electrode. This works direct research in the field of flexible electrodes and BP material as an anode for LIB [43].
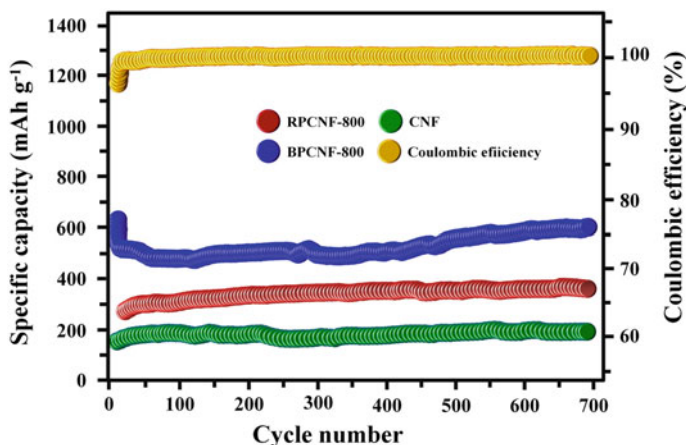
Fig. 14.13 Cycling performance of BPCNF-800, RPCNF-800 and CNFs at 1 A g^{-1} current density. Adapted and reproduced from Ref. [43], Copyright 2018 Elsevier

Table 14.1 Electrochemical performance of CNFs as anode for LIB

S. No.	Material	Surface area ($m^2 g^{-1}$)	Capacity (mAh g^{-1}), cycle number	Current density (mA g^{-1})	Reference
1	CNFs	NA	450, 2	30	[44]
2	Porous hollow CNF	13	501, 10	50	[45]
3	Free-standing N enriched porous CNF	1198	1150, 50	50	[40]
4	Black phosphorus-doped CNF (BPCNFs)	NA	607, 700	1000	[43]
5	N-doped porous CNF web	2381	943, 600	2000	[51]

Besides these, the porosity incorporation to CNF is also equally important to improve electrochemical performance of battery. Pores in CNF provide high surface area, more surface exposure for electrode/electrolyte interface and more charge transfer. In Table 14.1, papers reporting CNFs for LIB application are summarized with electrochemical performance. Though carbon is low cost, good cycling stability and lower electrochemical potential, its performance as an anode gives less reversible capacity value which turns in lower energy and power density. Hence, the development of nanocomposite of carbon with other high capacity materials like transition metal oxides/sulfides is a next step to achieve high capacity value with good cycling stability and high energy density. In the next section of chapter, transition metal oxides/sulfides and CNFs-based nanocomposites with their LIB performance are discussed.

14.4.2 CNFs-Based Nanocomposites as Anode for LIB

Metal-based anode materials provide more number of Li^+-ions involvement in electrochemical reaction as compared to commercially used graphite. Still, the utilization of these materials as anode in practical applications is not promising as it involves volume expansion during cycling, capacity fading and poor cycling stability. Various transition metal oxides (TMOs) including binary, ternary oxides have been researched as anode for LIB. Moreover, the nanoenginnering of metal oxides to get different morphology, alignment has been employed for better performance of oxides. However, the hurdle of low diffusion rate of Li^+-ion and poor electrical conductivity of metal oxides lowers the electrochemical performance and end in poor Li^+-ion storage [52]. To solve this issue, carbon may serve as support electrical conductivity

to TMOs. Out of different carbon morphologies, CNFs are most suitable candidate as 1D CNFs may control volume expansion caused in TMOs during electrochemical reactions.

High energy density, long cycle life as well as high rate capability is an essential parameter of Li^+-ion battery for the next generation electric vehicle and renewable energy storage device [53–55]. Current state-of-the-art graphite anode-based material is not able to meet the require energy density with their limited theoretical capacity of 372 mAh g^{-1}, and on the other hand, metal oxide has high theoretical capacity of >800 mAh g^{-1}. These metal oxides have one of the greatest problems of volume expansion and deformation of structural morphology resulting capacity fading [53, 56, 57]. To overcome of this problem and to get require essential energy density, one-dimensional carbon nanofiber and metal oxide-based composite are the possible and cheap way to improve the energy density. Also, it have several advantages including distinct electrical contact, high electron and Li^+-ion transport, unique electronic conduction, strain relaxation, outstanding durability and short diffusion pathways. Electrospun-based carbon nanofiber can prevent the integrating of metal oxide NPs, deterioration as well from volume expansion [58].

There are several electrospun-based syntheses have done for the CNF/metal oxide composite to meet the required amount of energy and power density. Fe_2O_3-based composite is one of the highly studied materials with CNF due to it has high theoretical capacity of 1005 mAh g^{-1}, natural abundance, low cost and environmental-friendly nature. Figure 14.14a shows the design and synthesis of bubbled-nanorod-structured Fe_2O_3-carbon nanofiber, which has been synthesized by Chao et al. [59] Another metal oxide which has been widely used as composite with CNF is SnO_2 because of the high theoretical capacity of 1494 mAh g^{-1}. Liu et al. has been synthesized SnO_x decorated CNF for the high performance LIBs [60]. There are several metal oxides, like Co_2O_3, CuO, SiO_2/Sb and TiO_2 have also been synthesized by different groups [59, 61–63]. One of the most excellent ideas to make CNF-based is to protect the volume expansion, cracking and crumbling of the electrode material resulting continual formation of unstable and insulating solid electrolyte interphase (SEI) layer, which are one of the reason for the loss of electric contact between electrode material and current collector as well as drastically capacity fading.

The electrochemical LIBs performance of Fe_2O_3 CNF has been shown in Fig. 14.15. The cyclic voltammogram of bubbled-nanorod-structure Fe_2O_3-C composite nanofiber is at 0.01 mV s^{-1}. The reduction peak observed at 0.7 V versus Li^+/Li which is due to reduction of Fe(III) to Fe (0), formation of Li_2O as well as irreversible reduction of electrolyte and formation of SEI layers. The appearance of the two anodic peaks at 1.5 and 1.8 V is because of the reversible oxidation of Fe (0) to Fe (II) and Fe (II) to Fe (III), respectively. Moreover, the peak at 0.5 V could be the partial decomposition of SEI layer. The hollow Fe_2O_3 and bubbled-nanorod-structured Fe_2O_3-C composite nanofiber are able to achieve initial first discharge and charge capacity of 1406 and 1145 mAh g^{-1}, 1335 and 1957 mAh g^{-1}, respectively.
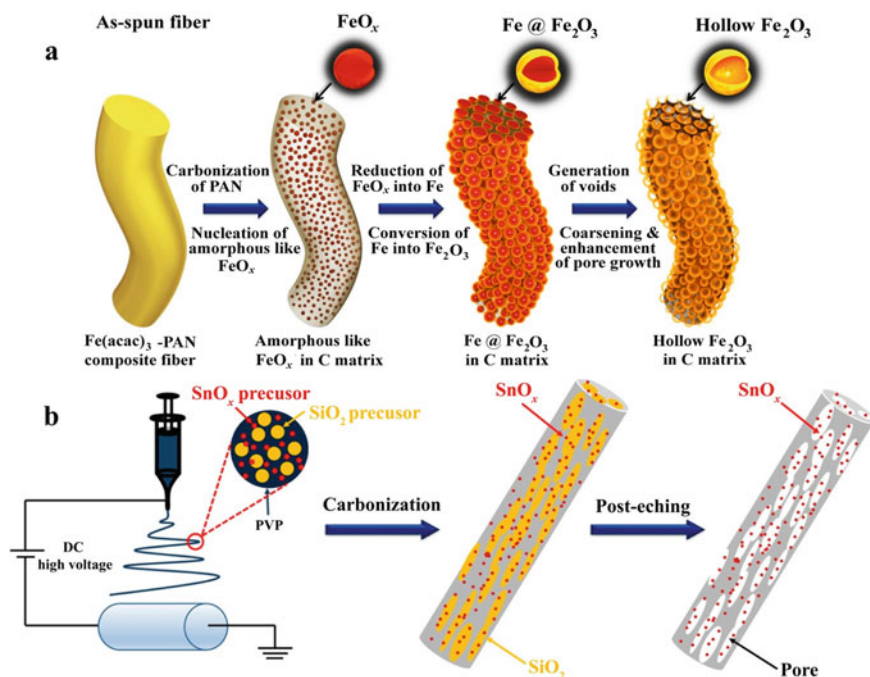
**Fig. 14.14 a** Synthesis of hollow Fe_2O_3 in C matrix, [59]. **b** SnO_x decorated porous carbon nanofibers. Adapted and reproduced from Ref. [60], Copyright 2016 American Chemical Society
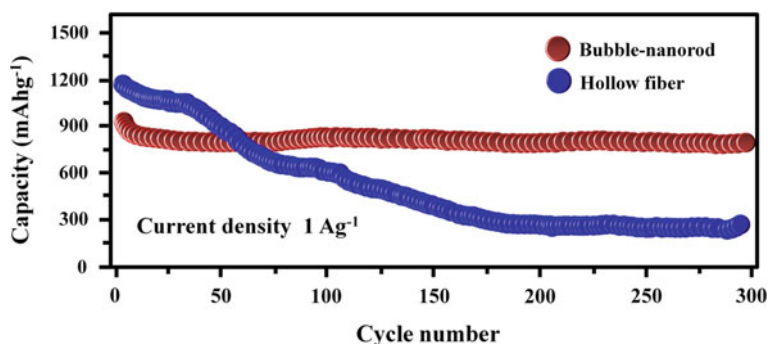
Fig. 14.15 Cyclic performance of bubbled-nanorod-structure Fe_2O_3-C composite nanofiber at 0.1 A g^{-1} Adapted and reproduced from Ref. [59], Copyright 2015 American Chemical Society

Figure 14.15 shows the stability of bubbled-nanorod-structured Fe_2O_3-C composite nanofiber at current density of 1 A g^{-1} up to 300 cycles. The initial capacity loss of first few cycles can be attributed to the partial destruction of the internal structure and decomposition of electrolyte as well as formation of the SEI layers.

The cyclic performance of three different compositions of SnO_x@PCNF and PCNF at 0.5 A g^{-1} is evaluated. Among all the samples, SnO_x@PCNF-2 has highest discharge capacity of 684 mAh g^{-1} and after 100 cycles retention capacity is 57.7%, and it exhibits rate performance with a reversible capacity of 819, 639, 468 and 323 mAh g^{-1} at a different current density of 0.2, 0.5, 1 and 2 A g^{-1}, respectively. Figure 14.16a, b shows charge and discharge capacity respectively for long cycle stability of SnO_x@PCNF-2 and even after 900 cycles the reversible capacity is 511 mA g^{-1}.
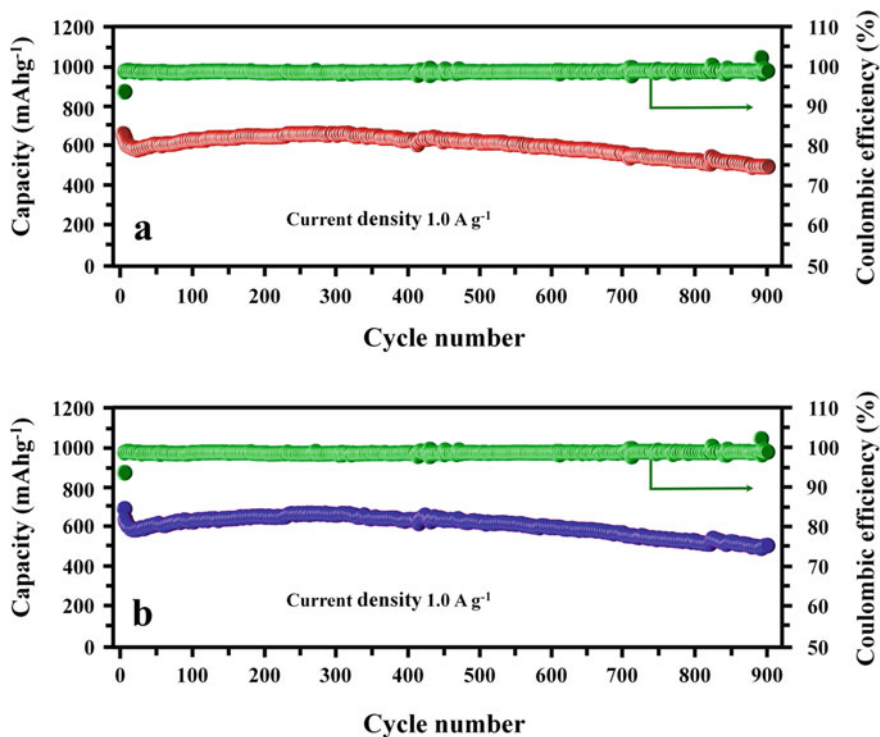

Fig. 14.16 **a** Charge capacity, **b** discharge capacity of SnO_x@PCNFs-2 for long term cycling at current density 1 A g^{-1} up to 900 cycles. Adapted and reproduced from Ref. [60], Copyright 2016 American Chemical Society

14.4.3 Transition Metal Sulfides Composites with Electrospun Carbon Nanofibers as Anodes for Lithium Ion Batteries

As discussed in the previous sections, there are several materials used as anodes for lithium ion batteries due to their interesting properties. As known, there are different types of anode materials such as insertion-type materials which are layered in structures and conversion-type anode materials which are generally transition metal oxides and then alloying type materials. However, interestingly, few materials participate both as insertion-type materials as well as conversion-type materials which has the advantage of gaining enhanced specific capacity. Here, we discuss few materials which are layered transition metal sulfides extensively explored for the LIBs as anode materials. Even though the transition metal sulfides participate as insertion-type and conversion-type materials they have few limitations and those needs to be addressed in order to make them commercially viable.

Transition metal sulfides have attracted huge attention as lithium ion batteries anode materials. Among these transition metal sulfides, MoS_2, WS_2, SnS and SnS_2 have a layered structure analogous to graphene. The single layer of these transition metal sulfides is formed as a sandwich of the transition metal atom (Mo, W) between the two sulfur atoms as shown in Fig. 14.17. Further, these single layers are bonded
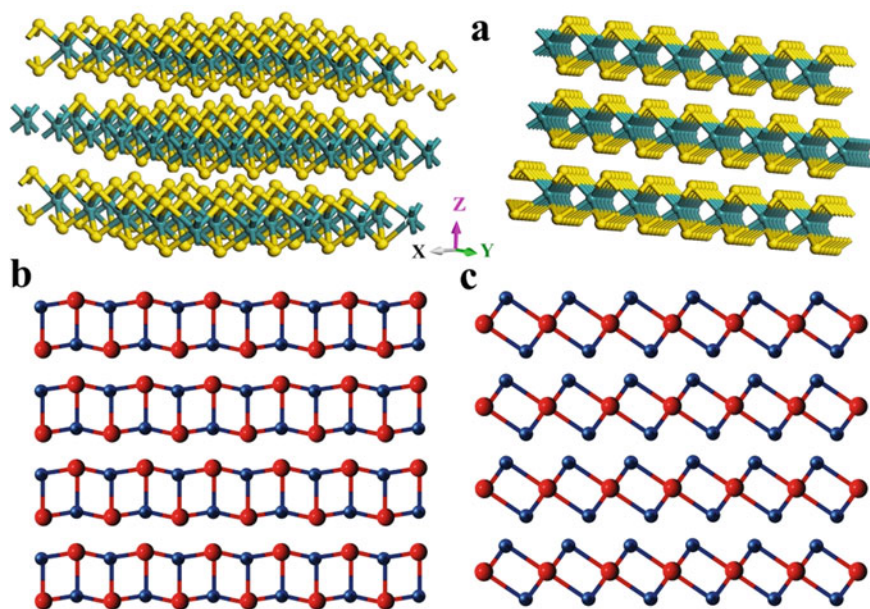
Fig. 14.17 Layered structure of **a** MoS_2. Adapted and reproduced from Ref. [67], Copyright 2020 Elsevier. **b** SnS_2 and SnS. **b** and **c** The blue balls are tin atoms, whereas the yellow balls are sulfur atoms. Adapted and reproduced from Ref. [68], Copyright 2017 Springer

to their adjacent layer through weak van der Waal's forces between the sulfur atoms [64]. And the atoms within the layer are bonded through a strong covalent bond. The layered nature of SnS and SnS_2 are also found to be akin to that of MoS_2 and WS_2 [65]. Since the layers of transition metal sulfides are bonded through week van der Waal's force, the Li^+-ions can easily undergo intercalation and de-intercalation to and from the layered structures, which is advantageous for the fast charging and discharging of the batteries based on these materials [66].

In the case of layered MoS_2, after intercalation of Li^+-ions into the MoS_2 layers, it undergoes conversion reaction to produce Li_2S and Mo [64] through the reaction-resulting in an increase in capacity. However, MoS_2 has poor electrical conductivity for the transfer of electrons; hence, for the fabrication of electrodes, one needs to add conductive carbons and polymeric binders. The polymeric binders being insulating in nature hinder the diffusion of ions and hence electron transfer. Therefore, it is very important to develop novel methods to design materials with good electrical conductivity as anodes for lithium ion batteries. Researchers have reported two methods to increase the specific capacity of MoS_2 and similar metal sulfides-based Li^+-ion batteries. One is to synthesize few-layered and even single-layered nanostructures of MoS_2, thereby reducing the strain developing during the intercalation of Li^+-ions. The second method is to synthesize MoS_2 coated with conductive carbon materials or composites of MoS_2 with conductive carbon nanostructures such as carbon nanotubes, carbon nanofibers, graphene, etc. [64]. In this expedition, there have been reports investigating the effect of making composites of MoS_2 and its nanostructures with carbon nanofibers synthesized by different methods. Here, we focus particularly on the composites of transition metal sulfides and its nanostructures with electrospun carbon nanofibers.

Electrospinning is a very useful technique to produce carbon nanofibers of varying aspect ratio and doping heteroatoms such as nitrogen, sulfur by using proper precursors. Electrospinning has been extensively used to synthesize carbon nanofibers and their composites with transition metal sulfides such as MoS_2, WS_2, SnS and SnS_2. We will discuss those works and try to understand the effect and advantages of making composites of electrospun carbon nanofibers with transition metal sulfides.

MoS_2 has a theoretical specific capacity of 670 mAh g^{-1} [66] which is much higher than that of graphite which is about 372 mAh g^{-1}. Hence, it is of very high interest to explore the possibilities to improve and use these materials from a commercialization point of view. However, in spite of having a high specific capacity MoS_2 does suffer from a few issues, such as poor electrical conductivity. Zhu et al. [64] reported the synthesis of nanoplates of MoS_2 embedded in carbon nanofibers using the precursors $(NH_4)_2MoS_4$ and polyvinylpyrrolidone in the required stoichiometry. They also point out that MoS_2 can undergo significant volume change during cycling of the cells. Hence, it is important to come up with a solution. Hence, they proposed and synthesized MoS_2 embedded in carbon nanofiber through electrospinning method which formed like a 3D network with the nanofiber diameter of around

50 nm. The thickness of the MoS_2 nanoplate thus obtained was 0.4 nm which shows the single-layered nature of the MoS_2 with a lateral dimension of 4 nm.

The TEM images of the MoS_2-nanoplate-CNF composite are shown in Fig. 14.18. For first cycle, with 1712 mAh g^{-1} and 1267 mAh g^{-1} discharge and charge capacity values, the coulombic efficiency is 74%. In the second cycle, the Coulombic efficiency increases to 95.5% and which increases to 99.1% after ten cycles. The
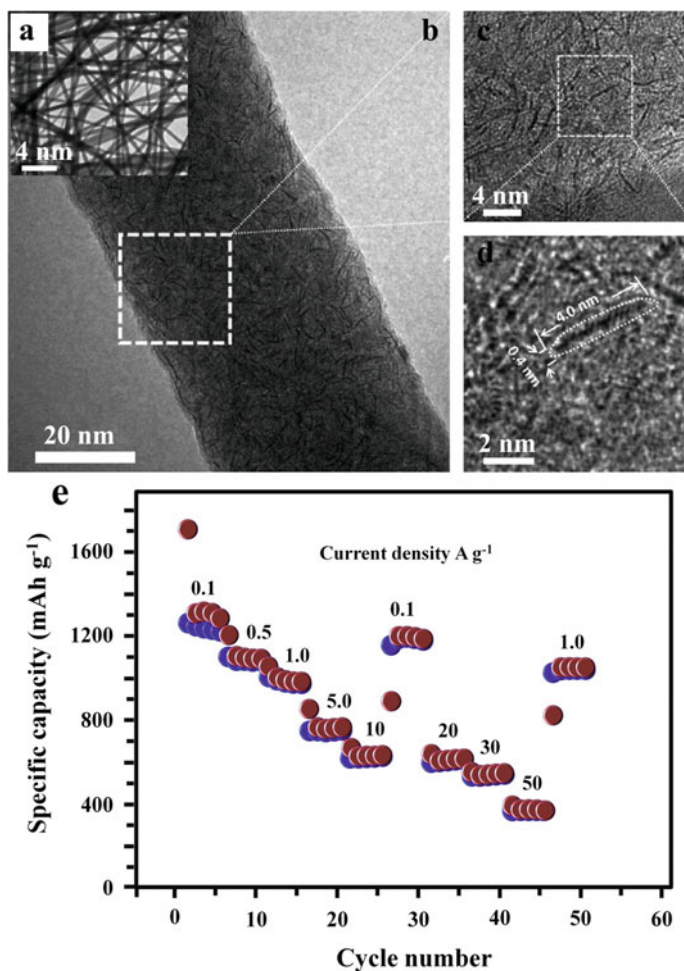

Fig. 14.18 **a** Bright-field TEM images of the MoS_2-CNF composites, **b** HRTEM image of the ultrathin MoS_2 on the surface of the CNF, **c**, **d** HRTEM images of marked region, **e** rate performance of MoS_2-CNF composites. Adapted and reproduced from Ref. [64], Copyright 2014 Wiley
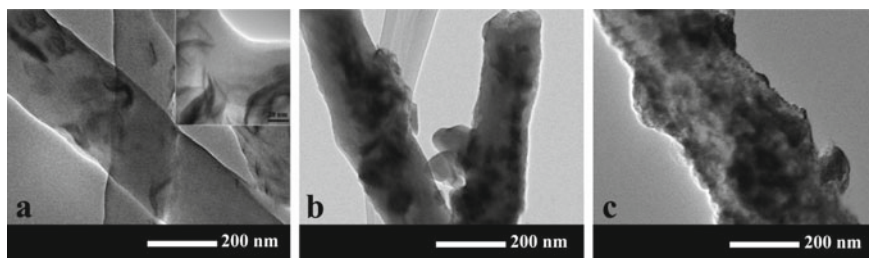
Fig. 14.19 a, b, c TEM images of MoS_2/C-47, MoS_2/C-73 and MoS_2/C-95, respectively. Adapted and reproduced from Ref. [69], Copyright 2014 American Chemical Society

composite also shows a remarkable rate capability of 374 mAh g^{-1} at 50 A g^{-1} together with excellent cycling stability of 661 mAh g^{-1} after 1000 cycles at a current density of 10 A g^{-1}. The authors ascribe this outstanding performance to the following; (1) the single layer nature of MoS_2 allows for the faster transport of the charge and storage through intercalation, conversion and alloying reactions. (2) The 1D nature of the carbon nanofibers helps easy access of ions.

Zhao et al. [69] synthesized MoS_2 nanoflakes encapsulated in carbon nanofibers prepared by electrospinning. They first synthesized MoS_2 nanoflakes by a solvothermal method and then dispersed different amounts of MoS_2 flakes 150, 300 and 900 mg in the precursor (PAN in DMF) for the synthesis of carbon nanofibers using single spinneret electrospinning technique at a voltage of 9.5–12.5 kV. Then, the obtained fibers were subjected to thermal treatment at steps to obtain carbon nanofibers. Thus, obtained nanofibers with MoS_2 nanoflakes were characterized with TEM which is shown in Fig. 14.19a–c. The authors then carried out electrochemical characterizations for the lithium ion batteries fabricated using the composite materials and the data is shown in Fig. 14.20a, b. In the cyclic voltammetry curve, the peak at 1.6 V in the cathodic part is attributed to the reduction of the oxygen and nitrogen-containing carbon obtained from the PAN. The slope appearing at 1.1 V indicates the
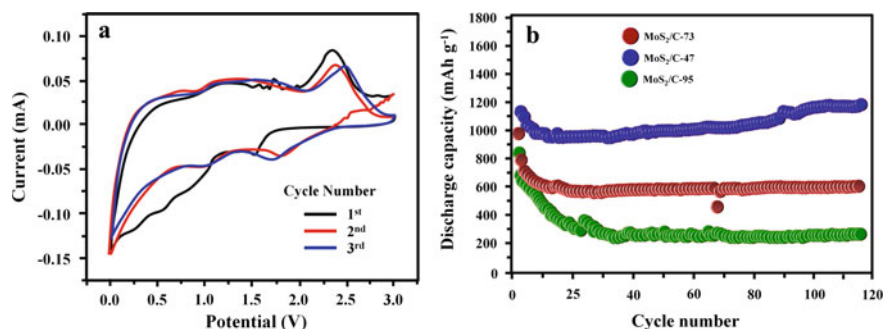
Fig. 14.20 a Cyclic voltammogram and (**b**) Cycling performance at 50 mA g^{-1} of prepared samples. Adapted and reproduced from Ref. [69], Copyright 2014 American Chemical Society

formation of the Li_xMoS_2 which then decomposes to Mo metal nanoparticles and Li_2S resulting in a cathodic peak at 0.5 V. Of the composites prepared with different loading of MoS_2, the one with 47% showed good cycling stability and rate capability. The sample delivered a capacity of 1133 mAh g^{-1} with a Coulombic efficiency of 73% at a current density of 50 mA g^{-1}. The excellent stability of the materials is resulting because of the confinement of the active material in the carbon matrix and the structural stability. Hence, the MoS_2 nanoflakes show very good performance as an anode material for the lithium ion batteries.

Yu et al. [70] reported the use of another transition metal sulfide tungsten disulfide (WS_2) single layer as an anode material in composite with nitrogen-doped carbon nanofiber (WS_2@NCNF) prepared by electrospinning. The composite materials were synthesized through a one-step synthetic route followed by heat treatment in two steps. WS_2 has a theoretical specific capacity of 433 mAh g^{-1} and the charge storage mechanism in this material is similar to MoS_2. That is, the lithium ions are stored as Li_2S and the electrons in the W in the metallic form. The material delivered a specific capacity of 590.4 mAh g^{-1} at a current density of 0.1 A g^{-1} with a Coulombic efficiency of 81.7% and exhibits capacity retention of 437.5 mAh g^{-1} after 200
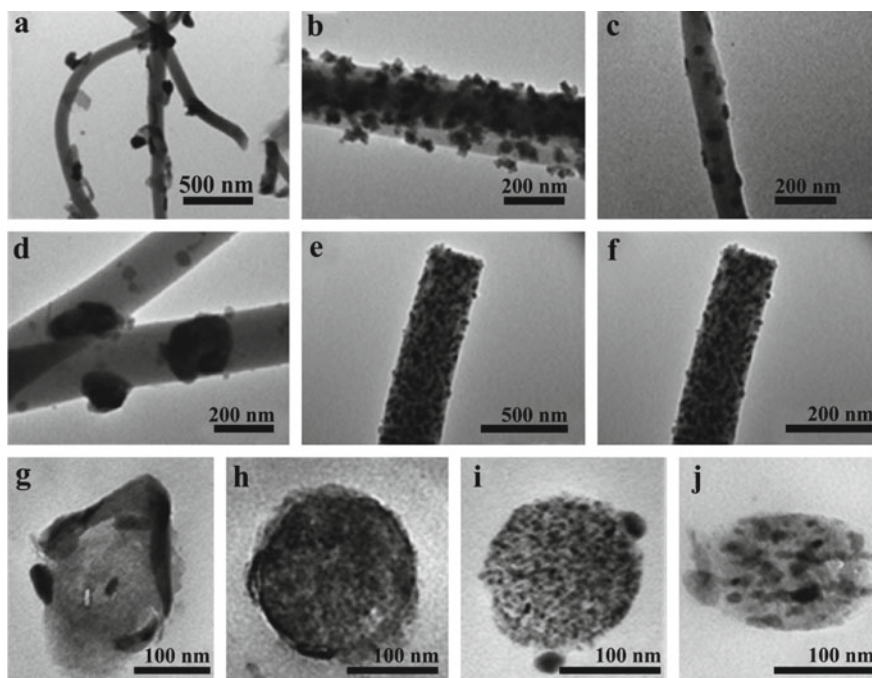
Fig. 14.21 TEM images of **a** $Cu_{1.96}S$@CNFs; **b** Co_9S_8@CNFs; **c** MnS@CNFs; **d** FeS@CNFs; **e** NiS@CNFs; **f** SnS@CNFs and microtomed cross section of **g** $Cu_{1.96}S$@CNFs; **h** MnS@CNFs; **i** NiS@CNFs; **j** SnS@CNFs. Adapted and reproduced from Ref. [71], Copyright 2016 Royal Society of Chemistry

cycles at 0.5 A g^{-1} current density and delivering a capacity of 367.1 mAh g^{-1} at 2 A g^{-1} which shows a very good rate capability. The cyclic voltammogram shows the characteristic peaks for the oxidation and reduction reactions. The reduction peak at 1.27 V represents the insertion of Li-ions into the WS$_2$, and the formation of Li$_x$WS$_2$ and the peak at 0.57 V has been ascribed to the conversion of Li$^+$-ions with the WS$_2$ and subsequent decomposition of the electrolyte. The peak at 0.57 V disappears after the first cycle and the peak at 1.27 V shifts to 1.83 V. The oxidation peaks appearing at 1.43 and 2.18 V represent the extraction of lithium from the WS$_2$. The reversible specific capacity of 590.4 mAh g^{-1} is higher than the theoretical specific capacity of the WS$_2$, this additional increase in capacity is ascribed to the contribution from the lithium storage at the interfaces of WS$_2$ nanoplates and formation of the W nanoparticles after the conversion reaction. The nitrogen-doped carbon nanofibers with improved electrical conductivity provide additional pathways for the electrons.

Fei et al. [71] reported the synthesis of different metal sulfides with carbon nanofibers using electrospinning by dispersing the sulfur into the solution of polymer and metal acetates and subjecting the obtained fibers to thermal treatment in the nitrogen gas environment This way the authors have synthesized SnS@CNFs, MnS@CNFs, FeS@CNFs, Cu$_{1.96}$S@CNFs, and Co$_9$S$_8$@CNFs, NiS@CNFs, and tested their lithium ion batteries performance as anode materials and the results are shown in Fig. 14.22. Their morphological studies have been depicted in Fig. 14.21. Out of all these composite samples, SnS@CNFs showed high capacity owing to the highest theoretical capacity of SnS together with high rate capability. The high performance and the excellent rate capability are attributed to the embedding of nanoparticles in the structure of the fiber which not only accommodates volume expansion but also prevents the aggregation of nanoparticles. The presence of a large number of micropores on the nanofibers allows for the fast diffusion of electrolyte and fast approach of the Li$^+$-ions to the metal sulfide particles.

Zhang et al. [72] designed graphene-wrapped carbon nanofibers and grew WS$_2$ nanosheets on them to improve the electrical conductivity and accommodate the large volume expansion and contraction during lithiation and de-lithiation. Graphene
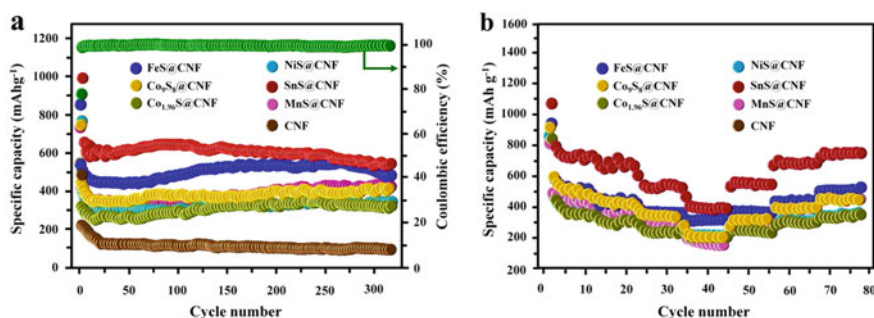

Fig. 14.22 **a** Cycling performance of the six samples and CNFs at a current density of 0.5 A g^{-1}; **b** rate performance of the six samples. Adapted and reproduced from Ref. [71], Copyright 2016 Royal Society of Chemistry
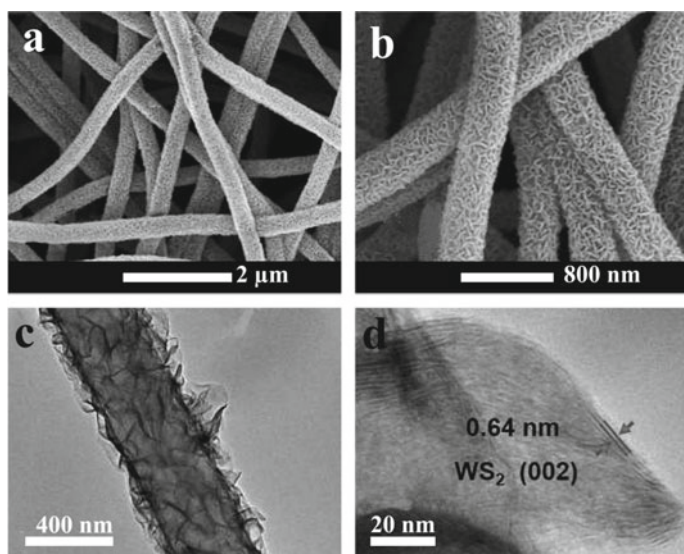
Fig. 14.23 Microstructures of WS$_2$/GCNF-2 hybrid membrane. **a**, **b** FESEM images, **c** TEM and **d** HRTEM images of WS$_2$/GCNF-2. Adapted and reproduced from Ref. [72], Copyright 2016 Royal Society of Chemistry

nanosheets were separately synthesized by the modified Hummer's method and the pre-oxidized polyacrylonitrile (PAN) nanofibers were synthesized by electrospinning. Later, the PAN were added to graphene oxide dispersion in water for 24 h and then rinsed, dried in a vacuum and carbonizing at 950 °C in nitrogen ambiance to get graphene-wrapped carbon nanofibers. WS$_2$/GCNF composite was synthesized by a solvothermal method. Figure 14.23a–d shows FESEM images and HRTEM images of the WS$_2$ nanoflakes grown on the graphene-wrapped CNF. The authors prepared WS$_2$/GCNF composites with varying amount of WS$_2$ loading on the fibers by varying the amount of the WS$_2$ precursor ((NH$_4$)$_2$WS$_4$) during synthesis and then carried out electrochemical tests on the lithium ion batteries fabricated using the same materials without adding any polymeric binder or conductive carbon to make the electrodes.

The electrochemical data is shown in Fig. 14.24a, b. Among the different weight ratios of WS$_2$/GCNF prepared, the composites with 74.6% of WS$_2$ (WS$_2$/GCNF-2) showed better performance compared to other composites with 54.8% (WS$_2$/GCNF-1) and 88.3% (WS$_2$/GCNF-3) of WS$_2$. The WS$_2$/GCNF-2 exhibits an initial discharge capacity of 1624.3 and 1128.2 mAh g^{-1} as compared to the only WS$_2$ which delivered a capacity of 1305.6 and 693.4 Ah g^{-1}. This enhancement in capacity is attributed to the effective dispersion of WS$_2$ nanosheets in the GCNF nanofibers. The GCNF also provided good stability to WS$_2$/GCNF as against poor stability of WS$_2$ nanosheets in which conductive carbon and polymeric binders were used. WS$_2$/GCNF-2 anode delivers high initial charge capacity of 1128.2 mAh g^{-1} and retention of 1068.5 mAh g^{-1} after 100 cycles which is quite a good result.
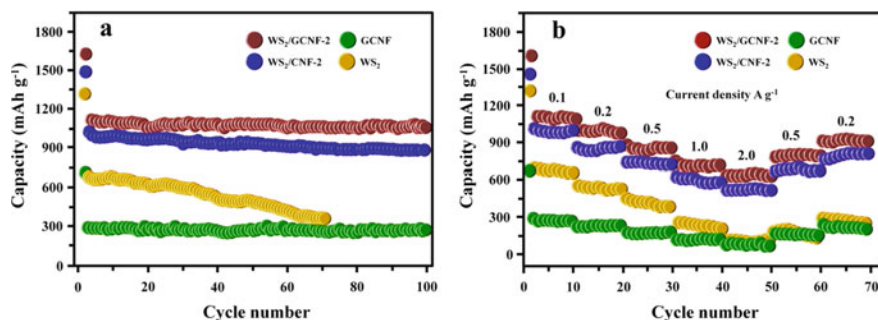
Fig. 14.24 **a** Cycling stability at 0.1 A g^{-1} and **b** rate performance of prepared samples. Adapted and reproduced from Ref. [72], Copyright 2016 Royal Society of Chemistry

Xia et al. [73] produced flexible and free-standing SnS/carbon nanofibers by dissolving suitable amounts of SnCl$_2$ and polyvinylpyrrolidone (PVP) in DMF and carrying out electrospinning. The electrospun fibers were then heated in a tube furnace in the presence of Ar/H$_2$ gas keeping thiourea in the upstream of the gas flow. The fibers obtained were again subjected to carbonization at different temperatures (550, 650 and 750 °C). Thus, the produced materials were used as anodes to fabricate binder and conductive carbon-free lithium ion batteries. The SnS has a layer spacing of 4.04 Å which is favorable for both Li$^+$ and Na$^+$-ion intercalation. The electrochemical characterization of the lithium ion batteries is shown in Fig. 14.25.

For the SnS/CNF prepared at 650 °C, in the cyclic voltammogram the peak at 0.98 V in the first cathodic curve is attributed to the conversion reaction of SnS with Li$^+$ to produce Li$_2$S and Sn which is given as SnS + 2Li$^+$ + 2e$^-$ → Sn + Li$_2$S. The peak at 0.54 V appears due to the formation of the solid electrolyte interface film. The peak appearing below 0.3 V may be representing the alloying reaction of Sn and
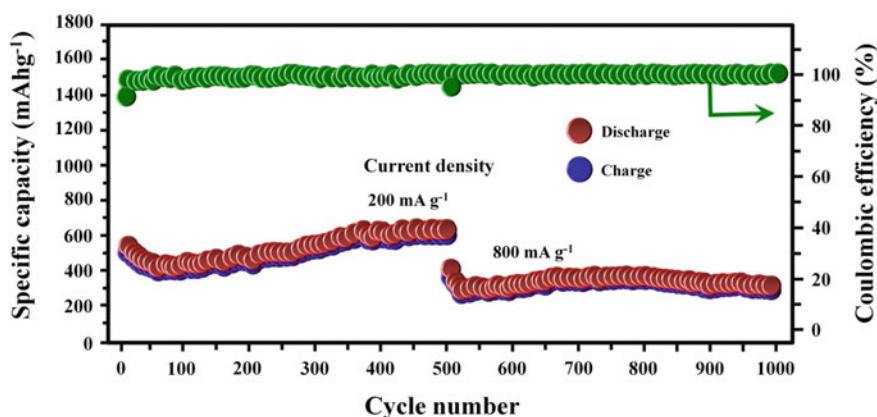
Fig. 14.25 Long-term cycling performance for SnS/C NFs-650 °C. Adapted and reproduced from Ref. [73], Copyright 2019 Elsevier

Li^+ ($Sn + xLi^+ + xe^- \rightarrow Li_xSn$ ($0 < x \le 4.4$), and the oxidations peaks occurring at 0.52 and 0.68 V show the multistep de-alloying processes. The first discharge and charge capacities of the materials are found to be 1278 mAh g^{-1} and 898 mAh g^{-1}, respectively, with a Coulombic efficiency of 70.3%, the loss in capacity could be due to electrolyte decomposition. Even at a current density of 4 A g^{-1}, the SnS/C NFs-650 °C electrodes deliver a capacity of 206 mAh g^{-1} which is a very good value. The SnS/C NFs-650 °C electrode also delivers an impressive higher capacity of 548 mAh g^{-1} even after 500 cycles while the other two deliver much lower capacity. The stable and improved performance of the SnS/C NFs-650 °C is observed to be due to the surface defect formed due to carbonization at 650 °C which favor more storage of Li$^+$-ions in the electrode. From these results, the authors conclude that the concentration of defects, electrical conductivity, and the amount of SnS present in the composite decides the capacity values obtained.

From all the above-discussed reports, we can understand that for the best performance of a given transition metal sulfide one needs to design proper composite which can improve the electrical conductivity, porosity, defects and the optimized content of the metal sulfide. With this in mind, one can design various possible metal sulfide electrospun carbon nanofiber composites for excellent performance as anode materials for lithium ion batteries.

14.5 Conclusion

In this chapter, we have discussed the synthesis of CNFs using electrospinning method. Wide varieties of material such as polymers, nanoparticles and composites have been employed to electrospinning to obtain nanofibers. Depending upon the need and current prospective, CNFs have been designed and functionalized by various materials. Although LIBs have been explored worldwide using graphite as anode material, yet to meet the demand of the next generation high energy and power density due to its limited theoretical capacity of 372 mAh g^{-1}. Hence, 1D CNF provides favorable properties for electrochemical storage of Li$^+$-ions in LIB through good access for electrolyte due to enhanced surface-volume ratio and conductivity along the length. High capacity and lower resistance are key electrochemical properties for CNFs as it provides shorter path length for Li$^+$ insertion and efficient 1D electron transport along length compared to powder materials. The varieties of nanomaterials such as CNF/metal oxides, CNF/metal sulfides, conducting polymers have been discussed along with their electrochemical performances. Also, advantages of high theoretical capacity materials as anodes for LIB and the challenges associated with it for composite making have been discussed with their Li$^+$-ion battery performance. The materials have been controllably, designed and synthesized as need of electrochemical view of points. Overall, the chapter summarized, designed and synthesis with unique strategies for the application of LIBs anode.

References

1. Marom R, Amalraj SF, Leifer N, Jacob D, Aurbach D (2011) A review of advanced and practical lithium batteries materials. J Mater Chem 21(27):9938–9954. https://doi.org/10.1039/c0jm04225k

2. Kim SW, Seo DH, Ma X, Ceder G, Kang K (2012) Electrode materials for rechargeable sodium-ion batteries: potential alternatives to current lithium ion batteries. Adv Energy Mater 2(7):710–721. https://doi.org/10.1002/aenm.201200026

3. Li W, Li M, Adair KR, Sun X, Yu Y (2017) Carbon nanofiber-based nanostructures for lithium-ion and sodium-ion batteries. J Mater Chem A 5(27):13882–13906. https://doi.org/10.1039/c7ta02153d

4. Chen XC, Wei W, Lv W, Su FY, He YB, Li B, Kang F, Yang QH (2012) A graphene-based nanostructure with expanded ion transport channels for high rate Li-ion batteries. Chem Commun 48(47):5904–5906. https://doi.org/10.1039/c2cc32276e

5. Reddy ALM, Shaijumon MM, Gowda SR, Ajayan PM (2009) Coaxial MnO_2/carbon nanotube array electrodes for high-performance lithium batteries. Nano Lett 9(3):1002–1006. https://doi.org/10.1021/nl803081j

6. Cui LF, Yang Y, Hsu CM, Cui Y (2009) Carbon–silicon core–shell nanowires as high capacity electrode for lithium ion batteries. Nano Lett 9(9):3370–3374. https://doi.org/10.1021/nl901670t

7. Weng W, Kurihara R, Wang J, Shiratori S (2019) Electrospun carbon nanofiber-based composites for lithium ion batteries: structure optimization towards high performance. Compos Commun 15:135–148. https://doi.org/10.1016/j.coco.2019.07.005

8. Zhang L, Aboagye A, Kelkar A, Lai C, Fong H (2014) A review: carbon nanofibers from electrospun polyacrylonitrile and their applications. J Mater Sci 49(2):463–480. https://doi.org/10.1007/s10853-013-7705-y

9. De Jong KP, Geus JW (2000) Carbon nanofibers: catalytic synthesis and applications. Catal Rev 42(4):481–510. https://doi.org/10.1081/CR-100101954

10. Inagaki M, Yang Y, Kang F (2012) Carbon nanofibers prepared via electrospinning. Adv Mater 24(19):2547–2566. https://doi.org/10.1002/adma.201104940

11. Zheng R, Zhao Y, Liu H, Liang C, Cheng G (2006) Preparation, characterization and growth mechanism of platelet carbon nanofibers. Carbon 44(4):742–746. https://doi.org/10.1016/j.carbon.2005.09.015

12. Tu JP, Zhu LP, Hou K, Guo SY (2003) Synthesis and frictional properties of array film of amorphous carbon nanofibers on anodic aluminum oxide. Carbon 41(6):1257–1263. https://doi.org/10.1016/S0008-6223(03)00047-2

13. Yu Y, Liu Y, Yang X (2016) Carbon nanofiber-based materials as anode materials for lithium ion batteries. InTech, 1, 978-953-51-2396-5, (3-30)

14. Kim MJ, Lee J, Jung D, Shim SE (2010) Electrospun poly (vinyl alcohol) nanofibers incorporating PEGylated multi-wall carbon nanotube. Synth Met 160(13–14):1410–1414. https://doi.org/10.1016/j.synthmet.2010.04.020

15. Wang P, Zhang D, Ma F, Ou Y, Chen QN, Xie S, Li J (2012) Mesoporous carbon nanofibers with a high surface area electrospun from thermoplastic polyvinylpyrrolidone. Nanoscale 4(22):7199–7204. https://doi.org/10.1039/c2nr32249h

16. Arshad SN, Naraghi M, Chasiotis I (2011) Strong carbon nanofibers from electrospun polyacrylonitrile. Carbon 49(5):1710–1719. https://doi.org/10.1016/j.carbon.2010.12.056

17. Ko Y, Kim J, Kim D, Kwon G, Yamauchi Y, You J (2019) Fabrication of highly conductive porous cellulose/PEDOT: PSS nanocomposite paper via post-treatment. Nanomaterials 9(4):612. https://doi.org/10.3390/nano9040612

18. Yang Y, Hou X, Ding C, Lan JL, Yu Y, Yang X (2017) Eco-friendly fabricated nonporous carbon nanofibers with high volumetric capacitance: improving rate performance by tri-dopants of nitrogen, phosphorus, and silicon. Inorg Chem Front 4(12):2024–2032. https://doi.org/10.1039/C7QI00517B

19. Kim C, Jeong YI, Ngoc BTN, Yang KS, Kojima M, Kim YA, Endo M, Lee JW (2007) Synthesis and characterization of porous carbon nanofibers with hollow cores through the thermal treatment of electrospun copolymeric nanofiber webs. Small 3(1):91–95. https://doi.org/10.1002/smll.200600243

20. McCann JT, Marquez M, Xia Y (2006) Melt coaxial electrospinning: a versatile method for the encapsulation of solid materials and fabrication of phase change nanofibers. Nano Lett 6(12):2868–2872. https://doi.org/10.1021/nl0620839

21. Yang HS, Lee BS, You BC, Sohn HJ, Yu WR (2014) Fabrication of carbon nanofibers with Si nanoparticle-stuffed cylindrical multi-channels via coaxial electrospinning and their anodic performance. RSC Adv 4(88):47389–47395. https://doi.org/10.1039/c4ra10031j

22. Kim C, Yang KS (2003) Electrochemical properties of carbon nanofiber web as an electrode for supercapacitor prepared by electrospinning. Appl Phys Lett 83(6):1216–1218. https://doi.org/10.1063/1.1599963

23. Wang Y, Serrano S, Santiago-Aviles JJ (2002) Conductivity measurement of electrospun PAN-based carbon nanofiber. J Mater Sci Lett 21(13):1055–1057. https://doi.org/10.1023/A:1016081212346

24. Zussman E, Chen X, Ding W, Calabri L, Dikin DA, Quintana JP, Ruoff RS (2005) Mechanical and structural characterization of electrospun PAN-derived carbon nanofibers. Carbon 43(10):2175–2185. https://doi.org/10.1016/j.carbon.2005.03.031

25. Dong L, Wang G, Li X, Xiong D, Yan B, Chen B, Li D, Cui Y (2016) PVP-derived carbon nanofibers harvesting enhanced anode performance for lithium ion batteries. RSC Adv 6(5):4193–4199. https://doi.org/10.1039/c5ra23924a

26. Ding B, Kim HY, Lee SC, Lee DR, Choi KJ (2002) Preparation and characterization of nanoscaled poly (vinyl alcohol) fibers via electrospinning. Fibers Polym 3(2):73–79. https://doi.org/10.1007/BF02875403

27. Son WK, Youk JH, Lee TS, Park WH (2005) Effect of pH on electrospinning of poly (vinyl alcohol). Mater Lett 59(12):1571–1575. https://doi.org/10.1016/j.matlet.2005.01.025

28. Hong SM, Kim SH, Jeong BG, Jo SM, Lee KB (2014) Development of porous carbon nanofibers from electrospun polyvinylidene fluoride for CO_2 capture. RSC Adv 4(103):58956–58963. https://doi.org/10.1039/c4ra11290c

29. Kim JR, Choi SW, Jo SM, Lee WS, Kim BC (2004) Electrospun PVdF-based fibrous polymer electrolytes for lithium ion polymer batteries. Electrochim Acta 50(1):69–75. https://doi.org/10.1016/j.electacta.2004.07.014

30. Zhao Z, Li J, Yuan X, Li X, Zhang Y, Sheng J (2005) Preparation and properties of electrospun poly (vinylidene fluoride) membranes. J Appl Polym Sci 97(2):466–474. https://doi.org/10.1002/app.21762

31. Yang Y, Centrone A, Chen L, Simeon F, Hatton TA, Rutledge GC (2011) Highly porous electrospun polyvinylidene fluoride (PVDF)-based carbon fiber. Carbon 49(11):3395–3403. https://doi.org/10.1016/j.carbon.2011.04.015

32. Ji L, Lin Z, Medford AJ, Zhang X (2009) Porous carbon nanofibers from electrospun polyacrylonitrile/SiO_2 composites as an energy storage material. Carbon 47(14):3346–3354. https://doi.org/10.1016/j.carbon.2009.08.002

33. Fan L, Yang L, Ni X, Han J, Guo R, Zhang CJ (2016) Nitrogen-enriched meso-macroporous carbon fiber network as a binder-free flexible electrode for supercapacitors. Carbon 107:629–637. https://doi.org/10.1016/j.carbon.2016.06.067

34. Zhang L, Jiang Y, Wang L, Zhang C, Liu S (2016) Hierarchical porous carbon nanofibers as binder-free electrode for high-performance supercapacitor. Electrochim Acta 196:189–196. https://doi.org/10.1016/j.electacta.2016.02.050

35. Peng YT, Lo CT (2015) Electrospun porous carbon nanofibers as lithium ion battery anodes. J Solid State Electrochem 19(11):3401–3410. https://doi.org/10.1007/s10008-015-2976-7

36. Niu H, Zhang J, Xie Z, Wang X, Lin T (2011) Preparation, structure and supercapacitance of bonded carbon nanofiber electrode materials. Carbon 49(7):2380–2388. https://doi.org/10.1016/j.carbon.2011.02.005

37. Zhang Z, Li X, Wang C, Fu S, Liu Y, Shao C (2009) Polyacrylonitrile and carbon nanofibers with controllable nanoporous structures by electrospinning. Macromol Mater Eng 294(10):673–678. https://doi.org/10.1002/mame.200900076

38. Heo YJ, Zhang Y, Rhee KY, Park SJ (2019) Synthesis of PAN/PVDF nanofiber composites-based carbon adsorbents for CO2 capture. Compos B Eng 156:95–99. https://doi.org/10.1016/j.compositesb.2018.08.057

39. Ju YW, Park SH, Jung HR, Lee WJ (2009) Electrospun activated carbon nanofibers electrodes based on polymer blends. J Electrochem Soc 156(6):A489–A494. https://doi.org/10.1149/1.3116245

40. Nan D, Huang ZH, Lv R, Yang L, Wang JG, Shen W, Lin Y, Yu X, Ye L, Sun H, Kang F (2014) Nitrogen-enriched electrospun porous carbon nanofiber networks as high-performance free-standing electrode materials. J Mater Chem A 2(46):19678–19684. https://doi.org/10.1039/c4ta03868a

41. Zhou T, Jiang Q, Wang L, Qiu Z, Liu Y, Zhou J, Liu B (2018) Facile preparation of nitrogen-enriched hierarchical porous carbon nanofibers by Mg(OAc)$_2$-assisted electrospinning for flexible supercapacitors. Appl Surf Sci 456:827–834. https://doi.org/10.1016/j.apsusc.2018.06.214

42. Chen LF, Lu Y, Yu L, Lou XWD (2017) Designed formation of hollow particle-based nitrogen-doped carbon nanofibers for high-performance supercapacitors. Energy Environ Sci 10(8):1777–1783. https://doi.org/10.1039/c7ee00488e

43. Li D, Wang D, Rui K, Ma Z, Xie L, Liu J, Zhang Y, Chen R, Yan Y, Lin H, Xie X (2018) Flexible phosphorus doped carbon nanosheets/nanofibers: electrospun preparation and enhanced Li-storage properties as free-standing anodes for lithium ion batteries. J Power Sources 384:27–33. https://doi.org/10.1016/j.jpowsour.2018.02.069

44. Kim C, Yang KS, Kojima M, Yoshida K, Kim YJ, Kim YA, Endo M (2006) Fabrication of electrospinning-derived carbon nanofiber webs for the anode material of lithium-ion secondary batteries. Adv Funct Mater 16(18):2393–2397. https://doi.org/10.1002/adfm.200500911

45. Lee BS, Son SB, Park KM, Lee G, Oh KH, Lee SH, Yu WR (2012) Effect of pores in hollow carbon nanofibers on their negative electrode properties for a lithium rechargeable battery. ACS Appl Mater Interfaces 4(12):6702–6710. https://doi.org/10.1021/am301873d

46. Hu C, Xiao Y, Zhao Y, Chen N, Zhang Z, Cao M, Qu L (2013) Highly nitrogen-doped carbon capsules: scalable preparation and high-performance applications in fuel cells and lithium ion batteries. Nanoscale 5(7):2726–2733. https://doi.org/10.1039/c3nr34002c

47. Wu Y, Fang S, Jiang Y (1998) Carbon anode materials based on melamine resin. J Mater Chem 8(10):2223–2227. https://doi.org/10.1039/A805080E

48. Endo M, Kim C, Karaki T, Nishimura Y, Matthews MJ, Brown SDM, Dresselhaus MS (1999) Anode performance of a Li ion battery based on graphitized and B-doped milled mesophase pitch-based carbon fibers. Carbon 37(4):561–568. https://doi.org/10.1016/S0008-6223(98)00222-X

49. Wu YP, Fang S, Jiang Y, Holze R (2002) Effects of doped sulfur on electrochemical performance of carbon anode. J Power Sources 108(1–2):245–249. https://doi.org/10.1016/S0378-7753(02)00013-7

50. Mao Y, Duan H, Xu B, Zhang L, Hu Y, Zhao C, Wang Z, Chen L, Yang Y (2012) Lithium storage in nitrogen-rich mesoporous carbon materials. Energy Environ Sci 5(7):7950–7955. https://doi.org/10.1039/c2ee21817h

51. Qie L, Chen WM, Wang ZH, Shao QG, Li X, Yuan LX, Hu XL, Zhang WX, Huang YH (2012) Nitrogen-doped porous carbon nanofiber webs as anodes for lithium ion batteries with a superhigh capacity and rate capability. Adv Mater 24(15):2047–2050. https://doi.org/10.1002/adma.201104634

52. Reddy MV, Subba Rao GV, Chowdari BVR (2013) Metal oxides and oxysalts as anode materials for Li ion batteries. Chem Rev 113(7):5364–5457. https://doi.org/10.1021/cr3001884

53. Zhang X, Liu H, Petnikota S, Ramakrishna S, Fan HJ (2014) Electrospun Fe$_2$O$_3$–carbon composite nanofibers as durable anode materials for lithium ion batteries. J Mater Chem A 2(28):10835–10841. https://doi.org/10.1039/c3ta15123a

54. Basavaraja BM, Majumder SB, Sharma A (2015) Electrospun hollow glassy carbon–reduced graphene oxide nanofibers with encapsulated ZnO nanoparticles: a free standing anode for Li-ion batteries. J Mater Chem A 3(10):5344–5351. https://doi.org/10.1039/c4ta07220k

55. Kim D, Lee D, Kim J, Moon J (2012) Electrospun Ni-added SnO_2–carbon nanofiber composite anode for high-performance lithium ion batteries. ACS Appl Mater Interfaces 4(10):5408–5415. https://doi.org/10.1021/am301328u

56. Zhang B, Huang J, Kim JK (2015) Ultrafine amorphous SnO_x embedded in carbon nanofiber/carbon nanotube composites for Li-ion and Na-ion batteries. Adv Funct Mater 25(32):5222–5228. https://doi.org/10.1002/adfm.201501498

57. Zhou X, Dai Z, Liu S, Bao J, Guo YG (2014) Ultra-uniform SnO_x/carbon nanohybrids toward advanced lithium ion batteries anodes. Adv Mater 26(23):3943–3949. https://doi.org/10.1002/adma.201400173

58. Wu Y, Zhu P, Reddy MV, Chowdari BVR, Ramakrishna S (2014) Maghemite nanoparticles on electrospun CNFs template as prospective lithium ion batteries anode. ACS Appl Mater Interfaces 6(3):1951–1958. https://doi.org/10.1021/am404939q

59. Cho JS, Hong YJ, Kang YC (2015) Design and synthesis of bubble-nanorod-structured Fe_2O_3–carbon nanofibers as advanced anode material for Li-ion batteries. ACS Nano 9(4):4026–4035. https://doi.org/10.1021/acsnano.5b00088

60. Liu Y, Yan X, Yu Y, Yang X (2016) Eco-friendly fabricated porous carbon nanofibers decorated with nanosized SnO_x as high-performance lithium ion batteries anodes. ACS Sustain Chem Eng 4(6):2951–2959. https://doi.org/10.1021/acssuschemeng.5b01236

61. Sahay R, Suresh Kumar P, Aravindan V, Sundaramurthy J, Chui Ling W, Mhaisalkar SG, Ramakrishna S, Madhavi S (2012) High aspect ratio electrospun CuO nanofibers as anode material for lithium ion batteries with superior cycleability. J Phys Chem C 116(34):18087–18092. https://doi.org/10.1021/jp3053949

62. Wang H, Yang X, Wu Q, Zhang Q, Chen H, Jing H, Wang J, Mi SB, Rogach AL, Niu C (2018) Encapsulating silica/antimony into porous electrospun carbon nanofibers with robust structure stability for high-efficiency lithium storage. ACS Nano 12(4):3406–3416. https://doi.org/10.1021/acsnano.7b09092

63. Zhang X, Suresh Kumar P, Aravindan V, Liu HH, Sundaramurthy J, Mhaisalkar SG, Duong HM, Ramakrishna S, Madhavi S (2012) Electrospun TiO_2–graphene composite nanofibers as a highly durable insertion anode for lithium ion batteries. J Phys Chem C 116(28):14780–14788. https://doi.org/10.1021/jp302574g

64. Zhu C, Mu X, van Aken PA, Yu Y, Maier J (2014) Single-layered ultrasmall nanoplates of MoS_2 embedded in carbon nanofibers with excellent electrochemical performance for lithium and sodium storage. Angew Chem Int Ed 53(8):2152–2156. https://doi.org/10.1002/anie.201308354

65. Wang L, Zhuo L, Yu Y, Zhao F (2013) High-rate performance of SnS_2 nanoplates without carbon-coating as anode material for lithium ion batteries. Electrochim Acta 112:439–447. https://doi.org/10.1016/j.electacta.2013.08.154

66. Xu X, Liu W, Kim Y, Cho J (2014) Nanostructured transition metal sulfides for lithium ion batteries: progress and challenges. Nano Today 9(5):604–630. https://doi.org/10.1016/j.nantod.2014.09.005

67. Nandi DK, Sen UK, Choudhury D, Mitra S, Sarkar SK (2014) Atomic layer deposited MoS_2 as a carbon and binder free anode in Li-ion battery. Electrochim Acta 146:706–713. https://doi.org/10.1016/j.electacta.2014.09.077

68. Xia C, Zhang F, Liang H, Alshareef HN (2017) Layered SnS sodium ion battery anodes synthesized near room temperature. Nano Research 10(12):4368–4377. https://doi.org/10.1007/s12274-017-1722-0

69. Zhao C, Kong J, Yao X, Tang X, Dong Y, Phua SL, Lu X (2014) Thin MoS_2 nanoflakes encapsulated in carbon nanofibers as high-performance anodes for lithium ion batteries. ACS Appl Mater Interfaces 6(9):6392–6398. https://doi.org/10.1021/am4058088

70. Yu S, Jung JW, Kim ID (2015) Single layers of WS_2 nanoplates embedded in nitrogen-doped carbon nanofibers as anode materials for lithium ion batteries. Nanoscale 7(28):11945–11950. https://doi.org/10.1039/c5nr02425k

71. Fei L, Williams BP, Yoo SH, Carlin JM, Joo YL (2016) A general approach to fabricate free-standing metal sulfide@carbon nanofiber networks as lithium ion batteries anodes. Chem Commun 52(7):1501–1504. https://doi.org/10.1039/c5cc06957b
72. Zhang L, Fan W, Liu T (2016) Flexible hierarchical membranes of WS_2 nanosheets grown on graphene-wrapped electrospun carbon nanofibers as advanced anodes for highly reversible lithium storage. Nanoscale 8(36):16387–16394. https://doi.org/10.1039/c6nr04241d
73. Xia J, Liu L, Jamil S, Xie J, Yan H, Yuan Y, Zhang Y, Nie S, Pan J, Wang X, Cao G (2019) Free-standing SnS/C nanofiber anodes for ultralong cycle-life lithium ion batteries and sodium-ion batteries. Energy Storage Mater 17:1–11. https://doi.org/10.1016/j.ensm.2018.08.005